

**A multiple spiking neural network architecture based on fuzzy intervals for anomaly detection
a case study of rail defects**

Phusakulkajorn, W.; Hendriks, J.M.; Moraal, J.; Dollevoet, R.P.B.J.; Li, Z.; Nunez, Alfredo

DOI

[10.1109/FUZZ-IEEE55066.2022.9882864](https://doi.org/10.1109/FUZZ-IEEE55066.2022.9882864)

Publication date

2022

Document Version

Final published version

Published in

2022 IEEE International Conference on Fuzzy Systems (FUZZ-IEEE)

Citation (APA)

Phusakulkajorn, W., Hendriks, J. M., Moraal, J., Dollevoet, R. P. B. J., Li, Z., & Nunez, A. (2022). A multiple spiking neural network architecture based on fuzzy intervals for anomaly detection: a case study of rail defects. In *2022 IEEE International Conference on Fuzzy Systems (FUZZ-IEEE)* (Vol. 2022). Article 1292 IEEE. <https://doi.org/10.1109/FUZZ-IEEE55066.2022.9882864>

Important note

To cite this publication, please use the final published version (if applicable).
Please check the document version above.

Copyright

Other than for strictly personal use, it is not permitted to download, forward or distribute the text or part of it, without the consent of the author(s) and/or copyright holder(s), unless the work is under an open content license such as Creative Commons.

Takedown policy

Please contact us and provide details if you believe this document breaches copyrights.
We will remove access to the work immediately and investigate your claim.

Green Open Access added to TU Delft Institutional Repository

'You share, we take care!' - Taverne project

<https://www.openaccess.nl/en/you-share-we-take-care>

Otherwise as indicated in the copyright section: the publisher is the copyright holder of this work and the author uses the Dutch legislation to make this work public.

A multiple spiking neural network architecture based on fuzzy intervals for anomaly detection: a case study of rail defects

Wassamon Phusakulkajorn, *Member, IEEE*, Jurjen Hendriks,
Jan Moraal, Rolf Dollevoet, Zili Li, and Alfredo Núñez, *Senior Member, IEEE*,

Abstract—In this paper, a fuzzy interval-based method is proposed for solving the problem of rail defect detection relying on an on-board measurement system and a multiple spiking neural network architecture. Instead of outputting binary values (defect or not defect), all data will belong to both classes with different spreads that are given by two fuzzy intervals. The multiple spiking neural networks are used to capture different sources of uncertainties. In this paper, we consider uncertainties in the parameters of spiking neural networks during the training phase. The proposed method comprises two steps. In the first step, multiple sets of the firing times for both classes are obtained from multiple spiking neural networks. In the second step, the obtained multiple sets of firing times are fuzzy numbers and they are used to construct fuzzy intervals. The proposed method is showcased with the problem of rail defect detection. The numerical analysis indicates that the fuzzy intervals are suitable to make use of the information provided by the multiple spike neural networks. Finally, with the proposed method, we improve the interpretability of the decision making regarding the detection of anomalies.

Index Terms—spiking neural network, parameter uncertainty, prediction interval, interpretability, anomaly detection.

I. INTRODUCTION

The performance of forecasting systems, control strategies and fault detection systems can be strongly affected by uncertainties in the processes. In addition, uncertainties in the model development are also of importance because they will affect the generalisation and predictive capability of the model, particularly when dealing with nonlinear processes.

Uncertainties in the model development can be classified into three types [1]. The first is model misspecification. It is uncertainty determined by how close the estimate model can approximate the real data under optimal parameter and data conditions. The second is uncertainty related to training data. It is uncertainty over how representative the training data is with respect to the whole input distribution, and how sensitive the model can be to unseen samples. The third is parameter uncertainty. It is uncertainty on the values of the model parameters due to local minimum stagnation. In this paper,

parameter uncertainty will be the main focus, particularly we will analyse the effect of synaptic weights.

In literature of neural networks, the estimation of synaptic weights is typically tackled by solving a non-convex optimisation problem. Thus, finding the global optimal parameters can not be guaranteed. To obtain a near optimal solution, multiple sets of synaptic weights are evaluated as the first estimation from which an optimisation algorithm searches for a better solution. As these weights are obtained from a random set of variables with a distribution defined a priori, it implies that there are many possible models in which some might be prone to local minimum stagnation.

The study of uncertainty quantification and its effects is crucial for the full understanding of the performance of the systems [2], [3]. Then, prediction interval arises as one of the techniques to represent effects of uncertainties over the future process behaviour [4]–[11]. Among the existing methods in the literature, fuzzy and fuzzy-neural interval models have been successfully used to quantify uncertainties in nonlinear systems from different research fields and applications [1], [12]. Some examples include waste-water treatment plants [13], modelling of the pH-titration curve [14], financial systems [6], [15], [16], biomedical engineering [17], renewable energy systems and microgrids [18]–[20], the solder paste deposition process [21], reactive power in electric arc furnace [22], aeronautics and astronautics [23], fault detection [24]–[26], among many others.

This paper investigates an effect of parameter uncertainty on anomaly detection using measurements of rail defects, a multiple spiking neural network (MSNN) architecture, and fuzzy intervals. In this paper, the dispersion of the firing times are considered and the firing times are generated from MSNNs whose synaptic weights are adjusted by backpropagation approach [27], [28] with multiple sets of random initial weights. To represent the most likely region to which the firing times will belong, the concept of fuzzy numbers is employed. Within these fuzzy intervals, a spread of firing times is analysed to obtain information that is used to define a classification rule and to quantify the prediction certainty of an anomaly detector based on MSNNs. Therefore, the decision regarding the detection of anomalies is interpretable. The dispersion of the output of the anomaly detector captured by the fuzzy intervals provides key information concerning uncertainty required in

W. Phusakulkajorn, J. Hendriks, J. Moraal, R. Dollevoet, Z. Li, and A. Núñez are with the Section of Railway Engineering, Delft University of Technology, 2628CN Delft, The Netherlands (e-mail:W.Phusakulkajorn@tudelft.nl; J.M.Hendriks@tudelft.nl; J.Moraal@tudelft.nl; R.P.B.J.Dollevoet@tudelft.nl; Z.Li@tudelft.nl; A.A.Nunezvicencio@tudelft.nl).

maintenance decision-making processes, making them more informative and accurate [29]–[31].

The rest of the paper is organised as follows. Section II introduces a multiple spiking neural network architecture based on fuzzy intervals for anomaly detection. The problem of rail defect detection is introduced as a case study to evaluate the method in Section III. The experimental analysis is elaborated in Section IV. Section V concludes the paper.

II. METHODOLOGY

Figure 1 presents a fuzzy interval based method that relies on an on-board measurement system and an MSNN architecture to solve the problem of anomaly detection. In this paper, MSNNs are used to capture uncertainties arising from the training phase due to random initial weights in a binary classification of the problem (nondefective and defective rails). The proposed method comprises two steps. In the first step, multiple sets of the firing times for both classes are obtained from MSNNs. In the second step, the obtained multiple sets of firing times are converted into fuzzy numbers and they are used to construct fuzzy intervals. With different spreads of firing times in both classes, the following information are obtained as outputs: an indication of the membership degree to each class and a predicted class label related to the fuzzy interval considering an estimation of the level of certainty.

A. Problem formulation

Anomaly detection can be considered as a classification problem. This problem assumes availability of a dataset $\mathcal{D} = \{(\mathbf{x}^{(b)}, c^{(b)}), b = 1, \dots, B\}$ containing pairs of an input $\mathbf{x}^{(b)} = [x_1^{(b)}, \dots, x_M^{(b)}] \in \mathbb{R}^M$ and its class label $c^{(b)} \in \{1, 2\}$, in which B is the number of pairs in \mathcal{D} and M is the number of features used to represent each input $\mathbf{x}^{(b)}$.

In this paper, the ground truth that relates an input $\mathbf{x}^{(b)}$ with its class label $c^{(b)}$ is obtained from experiments and fieldwork. In railways, collecting data and correctly labelling the samples of both defective and healthy states is costly, difficult, and time-consuming. It is costly because data are typically collected using specialised measurement trains and requires expert personnel with the know-how to evaluate the data. As rails are affected by local track dynamics and different stochastic variables, obtaining class information for both defective and healthy data is also difficult and time-consuming as typically field tests and additional measurements are required to confirm the presence of defects. These difficulties explain the large amount of data that is not being fully used by inframanagers, and the amount of unlabelled samples when dealing with railway data. Therefore, the goal in this paper is to provide a method that allows to obtain the correct class $c^{(b)}$ directly from $\mathbf{x}^{(b)}$ by capturing their relationship using fuzzy interval modelling together with an MSNN-based estimator.

Let \mathcal{G} be a set of spiking neural network-based estimators, $G_p, p = 1, \dots, P$, such that $G_p : \mathbf{x}^{(b)} \rightarrow \hat{c}_p^{(b)}$, in which $\hat{c}_p^{(b)}$ represents a predicted class label obtained from G_p . Given a dataset \mathcal{D} and a set of spiking neural network hyperparameters Θ , a set of synaptic weights of G_p is tuned to obtain a good

estimator of the problem. The tuning of these synaptic weights is a non-convex optimisation problem. Thus, these weights are initialised from multiple random variables and then optimised to obtain a near optimal solution using backpropagation. With the near-optimal synaptic weights W_p , each $G_p \in \mathcal{G}$ generates a corresponding set of firing times $\mathbf{F}_p = \{\hat{t}_1^p, \hat{t}_2^p\}$.

For all G_p , the obtained firing times of neuron j , $\hat{t}_j^p, p = 1, \dots, P, j = 1, 2$ are defined as fuzzy numbers and are used to define lower and upper bounds of the fuzzy interval $I_j = [\hat{t}_j^L, \hat{t}_j^U]$ for a class label j . Then, in this paper, based on the fuzzy intervals I_1 and I_2 , the percentage of prediction certainty is provided to improve the interpretability of the decision regarding the detection of anomalies. Then, we can define classification rules to predict the fuzzified output class label $c^{(b)}$ by making use of the multiple sets of firing times provided by the MSNN $\mathbf{F}_p, p = 1, \dots, P$ for every given input $\mathbf{x}^{(b)}$.

B. Multiple spiking neural networks

A spiking neural network (SNN) is considered as the third generation of neural networks [32]–[35]. It has been employed in fields such as biomedical science and mechanical engineering [36]–[39]. It processes and transmits information via trains of spiking events. For a given real-valued input $\mathbf{x} = [x_1, \dots, x_i, \dots, x_M]^T \in [0, 1]^M$, this paper employs the population rank encoding scheme with K receptive fields and the overlap constant set to 0.7 to convert each feature x_i into presynaptic spike times $\mathbf{t}_i = [t_i^1, \dots, t_i^K]^T \in [0, T]^K$ [28].

Compared to the other generations of neural networks, SNNs use spiking neurons as their computational units. In this paper, the spike times are processed in the presynaptic spiking neurons in which its spiking neuron model is based on the leaky-integrate-and-fire (LIF) model and the synaptic weights are time-varying [28], [40]. The membrane potential of each presynaptic spiking neuron has to be computed for a continuous duration of time to obtain the precisely timed patterns of spikes [33]. For the LIF neuron, a membrane potential $v_j(t)$ of the output neuron j is defined as the summation of a postsynaptic potential over the spike time k and the input feature i . Mathematically, a membrane potential $v_j(t)$ is expressed as:

$$v_j(t) = \sum_{i=1}^M \sum_{k=1}^K w_{ij}^k(t) \cdot \epsilon(t - t_i^k), \quad (1)$$

$$\epsilon(t) = \begin{cases} 0 & \text{if } t \leq 0, \\ \frac{t}{\tau} \exp(1 - \frac{t}{\tau}) & \text{if } t > 0, \end{cases} \quad (2)$$

where τ is the time constant of the spiking neuron and $w_{ij}^k(t) \in [0, T]$ is a time-varying synaptic weight that connects between the presynaptic neurons associated with the spike time k of the input feature i and the postsynaptic neuron j .

The information transmission of SNNs is based on the precise timing of spikes in addition to the number of spikes. The emission of spikes is allowed only when the membrane

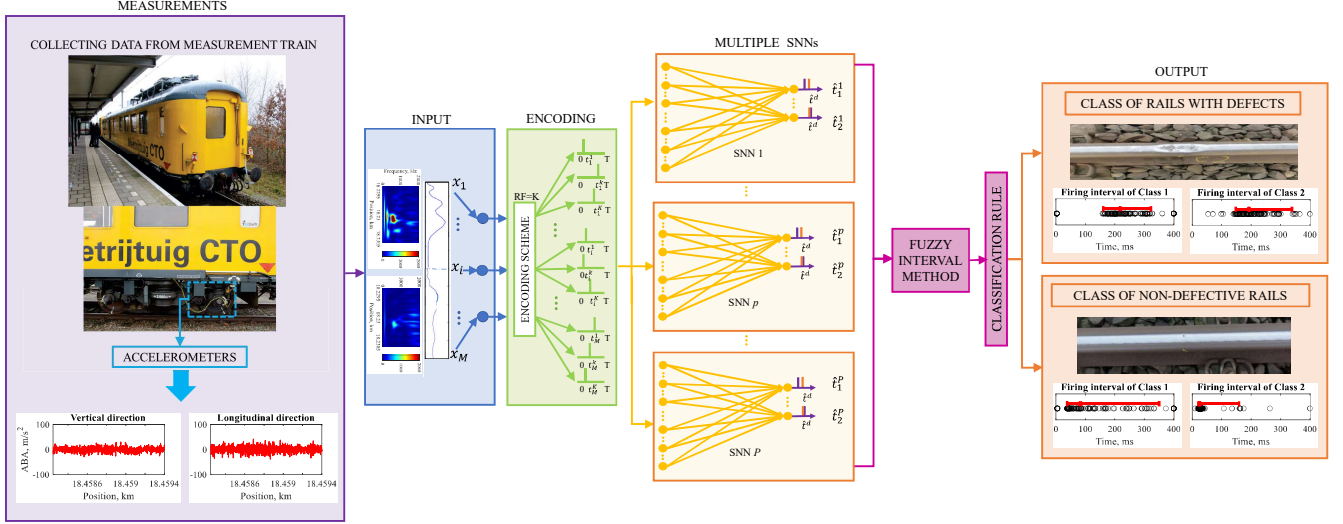


Fig. 1: The framework of the proposed fuzzy interval method based on multiple spiking neural networks for the detection of squats using ABA measurements.

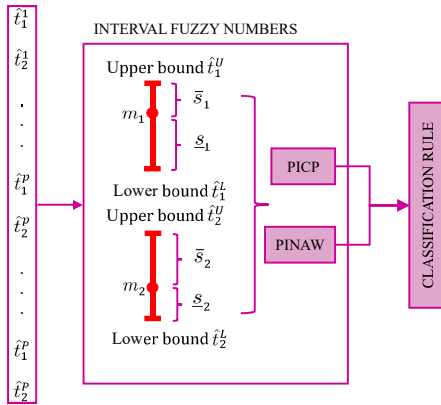


Fig. 2: Fuzzy interval method.

potential $v_j(t)$ reaches its firing threshold Λ . The postsynaptic firing time of neuron j , \hat{t}_j , is defined as:

$$\hat{t}_j = \{t | v_j(\hat{t}_j) = \Lambda\}. \quad (3)$$

At the postsynaptic firing time \hat{t}_j , the membrane potential of the neuron j is defined as:

$$\Lambda = v_j(\hat{t}_j) = \sum_{i=1}^M \sum_{k=1}^K w_{ij}^k(t) \cdot \epsilon(\hat{t}_j - t_i^k), \quad (4)$$

where \hat{t}_j lies in the postsynaptic spike time interval of $[0, T_{\text{sim}}]$ ms. The parameter T_{sim} represents the simulation time used for the internal potential to reach the threshold of the neuron. Its value is problem dependent.

For an SNN with the transmission type ruled by the time-to-first spike coding scheme, its output neuron can emit only once and its output associated with class j is the first postsynaptic

spike times \hat{t}_j . For a problem two classes, the classification rule to predict the output class label from the outputs $[\hat{t}_1, \hat{t}_2]^T$ for an input x is typically defined as:

$$\hat{c} = \arg \min_j \{\hat{t}_1, \hat{t}_2\}. \quad (5)$$

Suppose MSNN-based estimators, $G_p, p = 1, \dots, P$ are employed to capture parameter uncertainty due to random sets of initial weights in this paper, in which P is the number of SNNs. Therefore, the near-optimal synaptic weights $W_p = [w_{ij}^{k,p}(t), \dots, w_{ij}^{k,p}(t), \dots, w_{ij}^{k,p}(t)]^T$ of each G_p generates a set of firing times $F_p = \{\hat{t}_1^p, \hat{t}_2^p\}$, in which \hat{t}_j^p is the postsynaptic firing time of neuron j of $G_p, p = 1, \dots, P$ defined as:

$$\hat{t}_j^p = \{t | v_j^p(\hat{t}_j^p) = \Lambda\}, \quad (6)$$

and,

$$\Lambda = v_j^p(\hat{t}_j^p) = \sum_{i=1}^M \sum_{k=1}^K w_{ij}^{k,p}(t) \cdot \epsilon(\hat{t}_j^p - t_i^k). \quad (7)$$

Note that we are assuming the thresholds are the same; however, in more general settings, these thresholds can depend on the particular SNN, G_p . Our propose of using MSNNs is to capture different recommendations from different SNNs that contain different knowledge about the problem and provides information with different levels of certainties. To incorporate the diversity of information provided by MSNNs, a fuzzy interval method is considered. This is to select and capture useful information for the decision making process of anomaly detection.

C. Fuzzy interval method

With the concept of fuzzy numbers, the generated firing times \hat{t}_j^p are then defined as fuzzy numbers and are expressed

as a fuzzy interval. For the input $\mathbf{x}^{(b)}$, the fuzzy interval of firing times of neuron j is expressed as $I_j = [\hat{t}_j^{(b),L}, \hat{t}_j^{(b),U}]$, where $\hat{t}_j^{(b),L}$ and $\hat{t}_j^{(b),U}$ are the lower and upper bounds of the fuzzy interval, respectively.

To define the lower and upper bounds for class label j , the firing times of the respective neuron j are characterised by a mean m_j and a spread s_j such that $\hat{t}_j^{(b),L} = m_j^{(b)} - s_j^{(b)}$ and $\hat{t}_j^{(b),U} = m_j^{(b)} + s_j^{(b)}$ [18]. In this paper, a k^{th} percentile is proposed for identifying a mean and spreads. The 50th percentile is selected for the value of mean to address asymmetric distribution of the firing times, whereas different orders of percentile can be selected for a lower and upper bounds to provide a coverage probability of $(1 - \alpha)\%$ that future firing times under uncertain belong to the interval as:

$$\mathcal{P}(\hat{t}_j^{(b),L} \leq \hat{t}_j^{(b),p} \leq \hat{t}_j^{(b),U}) \geq (1 - \alpha)\%. \quad (8)$$

Then, the spread $s_j^{(b)} = [\underline{s}_j^{(b)}, \bar{s}_j^{(b)}]$ can be identified as:

$$\underline{s}_j^{(b)} = m_j^{(b)} - \hat{t}_j^{(b),L} \quad (9)$$

$$\bar{s}_j^{(b)} = \hat{t}_j^{(b),U} - m_j^{(b)}. \quad (10)$$

D. Performance metrics of fuzzy interval

For the concept of fuzzy numbers, the prediction interval coverage probability (PICP) and the prediction interval normalised average width (PINAW) are employed to quantitatively evaluate the quality of a fuzzy interval [18], [22]. The PICP provides the probability of firing times fall within the fuzzy interval. For a given dataset containing B samples, the PICP of class label j is mathematically expressed as:

$$\text{PICP}_j = \frac{1}{B} \sum_{b=1}^B \text{PICP}_j^{(b)}, \quad (11)$$

and,

$$\text{PICP}_j^{(b)} = \frac{1}{P} \sum_{p=1}^P a_p, \quad (12)$$

where a_p is a Boolean value calculated as:

$$a_p = \begin{cases} 1, & \text{if } \hat{t}_j^{(b),L} \leq \hat{t}_j^p \leq \hat{t}_j^{(b),U} \\ 0, & \text{otherwise.} \end{cases} \quad (13)$$

For the PINAW, it indicates the average width of the fuzzy interval. The PINAW of class label j is expressed as:

$$\text{PINAW}_j = \frac{1}{BR} \sum_{b=1}^B (\hat{t}_j^{(b),U} - \hat{t}_j^{(b),L}), \quad (14)$$

where R is the range of the firing times which is between 0 ms and T_{sim} ms.

E. Classification rule with percentage of certainty

For MSNNs $G_{p,p} = 1, \dots, P$, the classification rule to predict the output class label from the multiple sets of firing times $\mathbf{F}_p = \{\hat{t}_1^p, \hat{t}_2^p\}, p = 1, \dots, P$ is proposed based on fuzzy

intervals. For an input $\mathbf{x}^{(b)}$, its predicted class label $\hat{c}^{(b)}$ is expressed as:

$$\hat{c}^{(b)} = \arg \min_j \hat{t}_j^{(b),L}. \quad (15)$$

In this paper, the percentage of prediction certainty is proposed to quantify the decision uncertainty/certainty regarding the detection of anomalies using MSNNs. For class label j , the percentage of prediction certainty is defined as:

$$\frac{1}{P \times \text{PICP}_j^{(b)}} \sum_{p=1}^P \lambda_p \times 100, \quad (16)$$

where λ_p is a Boolean value calculated as:

$$\lambda_p = \begin{cases} 1, & \text{if } \hat{t}_j^{(b),L} \leq \hat{t}_j^{(b),p} \leq \hat{t}_j^{(b),L} \text{ and } a_p = 1 \\ 0, & \text{otherwise.} \end{cases} \quad (17)$$

III. CASE STUDY

A. Dataset

Data used in this paper are collected from axle box acceleration (ABA) measurements in both vertical and longitudinal directions covering approximately 1 kilometer of rails [41], [42]. The measurements are labelled according to experiments and fieldwork into two groups of non-defective rails and defective rails. There are a total of 662 rail samples, of which 577 samples are labelled as non-defective rail and 85 samples are labelled as defective rail. All samples in this paper are described by the 54 frequency-based representations of the measured ABAs [28]. They are assumed given in this paper.

B. Experimental setup

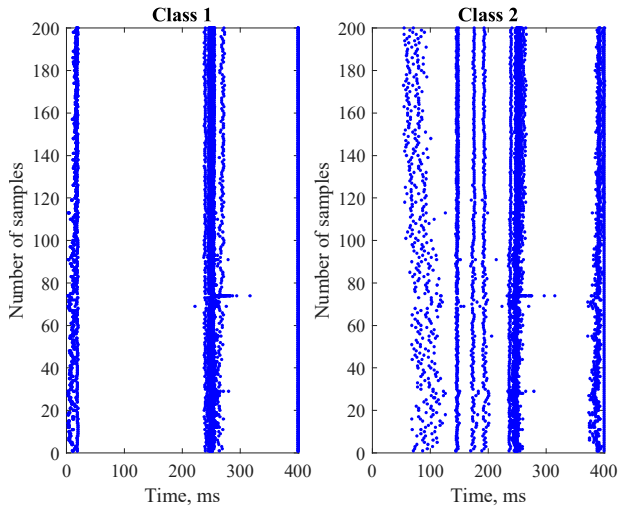
This paper considers a hundred SNNs. Each of them is designed with a two-layered fully connected feedforward architecture containing no hidden layers and no hidden nodes. After encoding input features by using 6 neurons with the Gaussian receptive fields, each network architecture consists of 324 input neurons and 2 output neurons associated with the class labels of the problem. The objective is to classify whether or not a given rail segment is defective. Therefore, a binary classification problem consists of a class of non-defective rails, referred to as Class 1, and a class of defective rails, referred to as Class 2.

The model parameters of each SNN comprise a group of hyperparameters and a group of synaptic weights. In this paper, parameter uncertainty is assumed to arise from only random sets of initial synaptic weights. For the hyperparameters, they include the time-varying weight kernel (σ), the desired postsynaptic firing time (\hat{t}^d), the time constant of spike response function (τ), and learning rate of weight update (η). Their values are assumed given as: $T = 3$, $T_{\text{sim}} = 4$, $\hat{t}^d = 2.46$, $\tau = 3.44$, $\sigma = 0.21$, and $\eta = 0.000248$. These are optimal values for the dataset obtained from sensitivity analysis reported in [28]. Using the given rail samples and value of hyperparameters, the synaptic weights of all SNNs are adjusted based on backpropagation with multiple sets of random initial weights. All models $G_{p,p} = 1, \dots, 100$ are

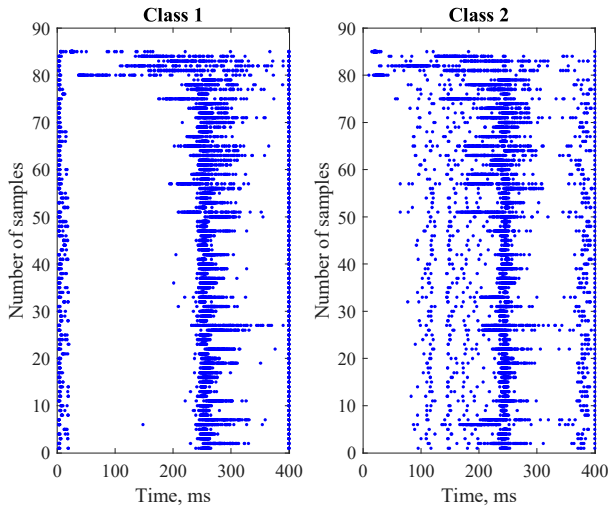
trained with 100 epochs, which has shown to be sufficient based on the experimental data.

IV. EXPERIMENTAL ANALYSIS

After training the MSNNs, $G_p, p = 1, \dots, 100$, a hundred sets of firing times $\{\mathbf{F}_1, \dots, \mathbf{F}_p, \dots, \mathbf{F}_{100}\}$ are obtained. Figure 3 illustrates a hundred sets of firing times of Class 1 and Class 2 for nondefective rails (see Figure 3a) and defective rails (see Figure 3b). It is observed that the firing times are more scattered in samples of defective rails than those of nondefective rails. This is the knowledge about the detection problem that the MSNNs are providing as a group. The firing times for Class 1 and Class 2 from samples of both rail groups are consistent when analysing each SNN. This consistency is exploited by defining the fuzzy intervals of each class.



(a) For 200 samples of non-defective rails.



(b) For all samples of defective rails.

Fig. 3: Distribution of firing times obtained from $G_p, p = 1, \dots, 100$ of Class 1 and Class 2.

For each sample b , the corresponding fuzzy intervals can be obtained from specifying an order of percentile of its firing times $\hat{t}_j^{(b),p}, p = 1, \dots, 100$ for the lower and upper bounds for Class 1 and Class 2. In this paper, a sensitivity analysis of the order of percentile to determine the fuzzy bounds was conducted. For this particular dataset, the construction of the fuzzy interval for Class 1 and Class 2 was defined by setting $\hat{t}_1^{(b),U}$ at 92th percentile and $\hat{t}_2^{(b),U}$ at 94.5th percentile, Figure 4 presents the effect of changing orders of percentile used to determine $\hat{t}_j^{(b),L}, j = 1, 2$ on the accuracy of the proposed method for predicting nondefective and defective rails. It is evident that different orders of percentile provide different prediction accuracy for both rail groups. For example, by selecting $\hat{t}_1^{(b),L}$ at the 9th percentile and $\hat{t}_2^{(b),L}$ at the 8th percentile, 96% of defective and 68% of nondefective rails are correctly predicted.

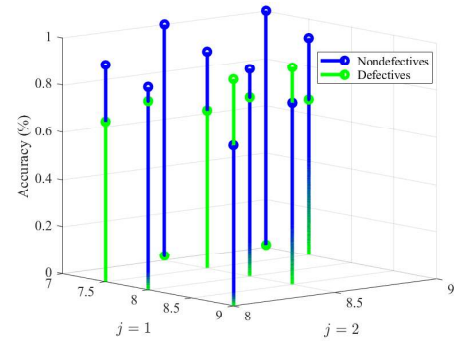
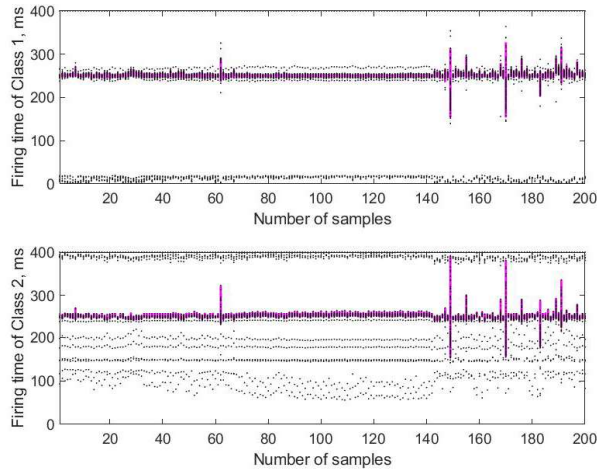


Fig. 4: Effect of changing order of percentile used to determine $\hat{t}_j^{(b),L}, j = 1, 2$ on the performance of the proposed method.

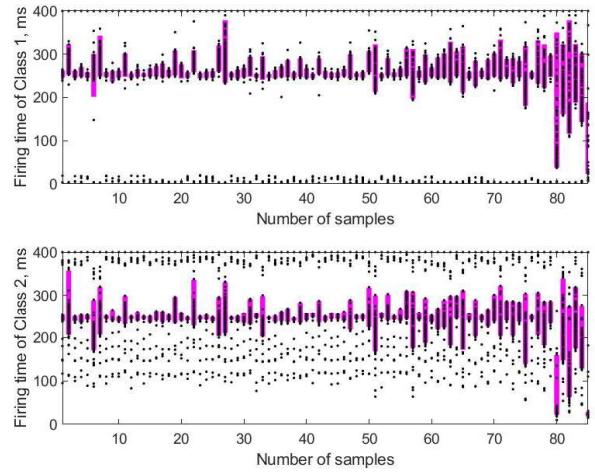
To showcase, we consider that $I_1^{(b)}, \forall b \in \mathcal{D}$ are constructed such that $\hat{t}_1^{(b),L}$ and $\hat{t}_1^{(b),U}$ is at the 9th and 92th percentile, respectively. And, $I_2^{(b)}, \forall b \in \mathcal{D}$ are constructed such that the $\hat{t}_2^{(b),L}$ is set at the 8th percentile and $\hat{t}_2^{(b),U}$ at 94.5th percentile. Using the specified intervals, Figure 5 illustrates the comparative plot of $I_1^{(b)}$ and $I_2^{(b)}$ (magenta bars) along with the obtained firing times (black dots) from samples of nondefective and defective rails.

To evaluate the quality of the constructed fuzzy intervals, the PICP and the PINAW of Class $j, j = 1, 2$ are analysed for all samples b . It is demonstrated in Figure 6 that the constructed fuzzy intervals $I_1^{(b)}$ and $I_2^{(b)}$ provide a reasonable coverage of the firing times produced by the neuron of Class 1 and Class 2. Both $I_1^{(b)}$ and $I_2^{(b)}$ cover similar probability between 0.86 and 0.89. It can be noticed that the values of $\text{PINAW}_1^{(b)}$ and $\text{PINAW}_2^{(b)}$ of nondefective rails are relatively smaller than those of defective rails for all sample b of the respective class. This reflects the high variability of the firing times of defective samples (see Figure 3(b)) which can infer that they are relatively more sensitive to the existing uncertainties than the samples of non-defective rails.

The predictive performance of the fuzzy intervals is investigated for rail anomaly detection by comparing to [28] where 96.67% of defective and 90.30% of nondefective rails were



(a) For 200 samples of non-defective rails.



(b) For all samples of defective rails.

Fig. 5: Illustration of the firing intervals $I_1^{(b)}$ and $I_2^{(b)}$ (magenta bars) along with the obtained firing times (black dots).

TABLE I: Comparative prediction between the proposed method and the method in [28]. NB: ND stands for nondefective and D stands defective.

Sample b	Fuzzy interval		PICP		PINAW		Class label			
	$I_1^{(b)}$	$I_2^{(b)}$	PICP $_1^{(b)}$	PICP $_2^{(b)}$	PINAW $_1^{(b)}$	PINAW $_2^{(b)}$	Actual	Predicted by		
								[28]	This paper	%certainty
1	[246.18,252.00]	[245.00,254.78]	0.85	0.87	5.82	9.78	ND	D	D	5.68
2	[246.00,254.00]	[247.00,258.73]	0.86	0.87	8.0	11.73	ND	ND	ND	3.44
3	[246.00,255.00]	[247.00,258.84]	0.86	0.87	9.0	11.84	ND	ND	ND	3.44
4	[244.95,253.42]	[245.58,254.95]	0.83	0.86	8.47	9.37	ND	D	ND	16.0
5	[246.36,254.42]	[245.00,250.95]	0.83	0.87	8.06	5.95	ND	D	D	79.54
⋮	⋮	⋮	⋮	⋮	⋮	⋮	⋮	⋮	⋮	⋮
658	[37.59,350.38]	[22.00,159.57]	0.83	0.89	312.79	137.57	D	D	D	95.56
659	[161.00,322.94]	[147.74,338.80]	0.84	0.86	161.94	191.06	D	D	D	13.79
660	[116.13,378.40]	[62.58,274.89]	0.83	0.86	262.27	212.31	D	D	D	77.01
661	[143.36,302.26]	[129.00,275.24]	0.83	0.87	158.9	146.24	D	D	D	21.59
662	[23.00,188.52]	[19.00,28.00]	0.84	0.89	165.52	9.0	D	D	D	88.89

correctly predicted. For the chosen fuzzy intervals (Figure 4), the prediction accuracy is relatively 0.69% less for defective and 24.70% less for non-defective rails. Please note that the predictive performance of our method based on fuzzy intervals is expected to be improved when the fuzzy intervals are optimally constructed. However, more interpretability of anomaly detection of rails is provided by the proposed fuzzy interval method. This is to elaborate in what follows.

Table I presents the predicted class label with a percentage of prediction certainty and the fuzzy intervals $I_1^{(b)}$ and $I_2^{(b)}$ for the selected samples b . It can be noticed that the class label of samples 658th and 659th is both correctly predicted by the proposed fuzzy interval method but with different percentage of prediction certainty. As sample 658th provides higher percentage of prediction certainty than that of sample 659th, it is observed from Figures 7(a) and 7(b) that the firing times $\hat{t}_2^{(658),p}$, $p = 1, \dots, 100$ are less spread within $I_2^{(658)}$ and more concentrated around its mean. For a single optimised SNN obtained in [28], it is shown that its firing time of the predicted class label is in a closer proximity to the mean of

the firing times obtained from this paper when a percentage of prediction certainty is higher.

In the case of sample 4th where the prediction result do not agree with that of [28], it is correctly predicted as a nondefective rail with 16% certainty. The lower percentage is explained in Figure 8 where both firing times $\hat{t}_1^{(4),p}$ and $\hat{t}_2^{(4),p}$, $p = 1, \dots, 100$ are concentrated around its respective mean. Unlike [28], the level of prediction certainty from the fuzzy intervals provides an interpretability for human operators in order to make final decision whether it is a defective/non-defective rail. Therefore, the spread of the firing times around the mean of the predicted class label and the value of PINAW play a role as an indication of decision uncertainty in anomaly detection using MSNNs. Further analysis can be conducted of those defective samples where a low certainty is obtained, so to tailor methods that explicitly handle those particular cases.

V. CONCLUSIONS

This paper has presented a fuzzy interval method based on a multiple spiking neural network architecture for anomaly

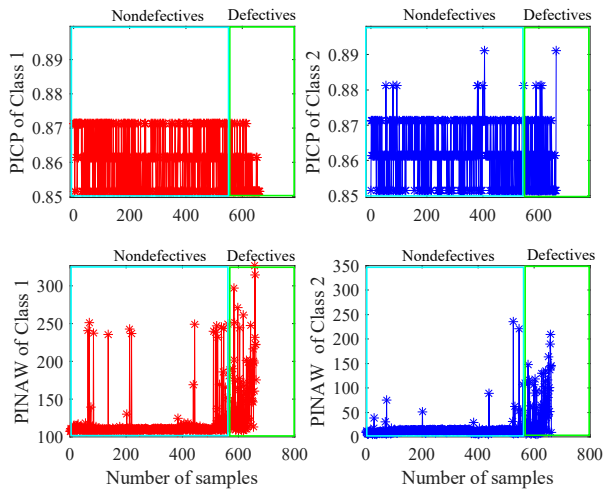
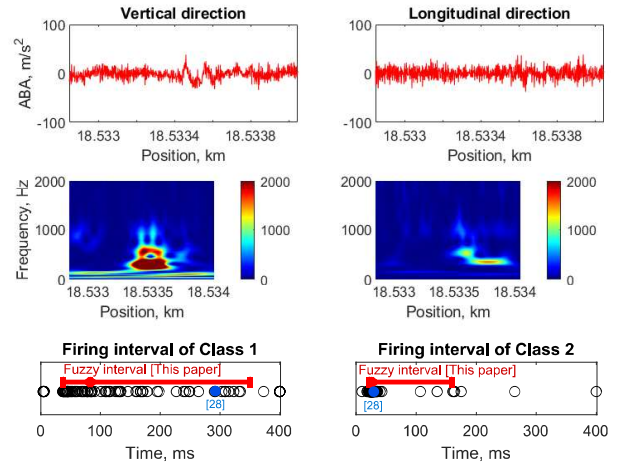


Fig. 6: The value of $\text{PICP}_j^{(b)}$ and $\text{PINAW}_j^{(b)}$ of Class j , $j = 1, 2$ when setting $\hat{t}_1^{(b),L}$ at the 9th percentile and $\hat{t}_2^{(b),L}$ at the 8th percentile.

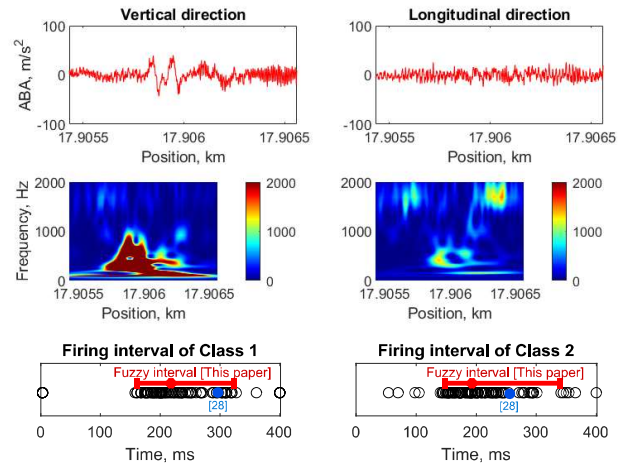
detection. The concept of fuzzy numbers is employed to construct fuzzy intervals of firing times generated from multiple spiking neural networks. The intervals are to represent the effect of uncertainties over anomaly detection with new dataset of different behaviour. The fuzzy interval method is evaluated with the problem of rail defect detection considering only uncertainty from the training phase due to random initial weights. With our selection of spread values of the fuzzy intervals, the experimental results show that the corresponding fuzzy intervals for the firing times of a neuron associated with Class 1 and Class 2 provide a reasonable coverage probability. The intervals can be used to detect 96% of defective and 68% of nondefective rails. This proves our idea that information carried via firing times of certain SNNs can be selected and included in the decision making process of the model. Using fuzzy intervals to express these information, an interpretability of anomaly detection confidence is improved. It is concluded that the more concentrated around the mean of the predicted class label and the lower the value of PINAW, the more certain the prediction. For future work, a multi-spiking neural network architecture will be used to capture more sources of uncertainty and to provide the respective supervision knowledge of rail squats. Then, we will work on multi-objective optimisation to maximise predictive performance and minimise spread values of the firing times representing necessary knowledge learned by the multi-spiking neural networks that should be included into the decision making process for anomaly detection.

REFERENCES

- [1] O. Cartagena, S. Parra, D. Muñoz-Carpintero, L. G. Marín, and D. Sáez, "Review on fuzzy and neural prediction interval modelling for nonlinear dynamical systems," *IEEE Access*, vol. 9, pp. 23 357–23 384, 2021.
- [2] A. Gray, A. Wimbush, M. de Angelis, P. Hristov, D. Calleja, E. Miralles-Dolz, and R. Rochetta, "From inference to design: A comprehensive framework for uncertainty quantification in engineering with limited



(a) Sample 658th that is correctly predicted as a defective rail with 95.56% of prediction certainty.



(b) Sample 659th that is correctly predicted as a defective rail with 13.79% of prediction certainty.

Fig. 7: Predictive result of two defective rails that have different percentages of prediction certainty.

- information," *Mechanical Systems and Signal Processing*, vol. 165, p. 108210, 2022.
- [3] M. Abdar, F. Pourpanah, S. Hussain, D. Rezazadegan, L. Liu, M. Ghavamzadeh, P. Fieguth, X. Cao, A. Khosravi, U. R. Acharya, V. Makarenkov, and S. Nahavandi, "A review of uncertainty quantification in deep learning: Techniques, applications and challenges," *Information Fusion*, vol. 76, pp. 243–297, 2021.
- [4] A. Khosravi, S. Nahavandi, D. Creighton, and A. F. Atiya, "Comprehensive review of neural network-based prediction intervals and new advances," *IEEE Transaction on Neural Networks*, vol. 22, pp. 1341–1356, 2011.
- [5] J. M. Mendel, *Uncertain rule-based fuzzy logic systems: Introduction and new directions (2nd ed.)*. Springer International Publishing, 2017.
- [6] D. Leite, P. Costa, and F. Gomide, *Interval Approach for Evolving Granular System Modeling*. New York, NY: Springer New York, 2012, pp. 271–300.
- [7] R. Babuška, "Fuzzy modeling for control (1st ed.)," *Boston, USA: Kluwer Academic Publishers.*, 1998.
- [8] M. Khodayar, J. Wang, and M. Manthouri, "Interval deep generative neural network for wind speed forecasting," *IEEE Transactions on Smart Grid*, vol. 10, pp. 3974–3989, 2019.

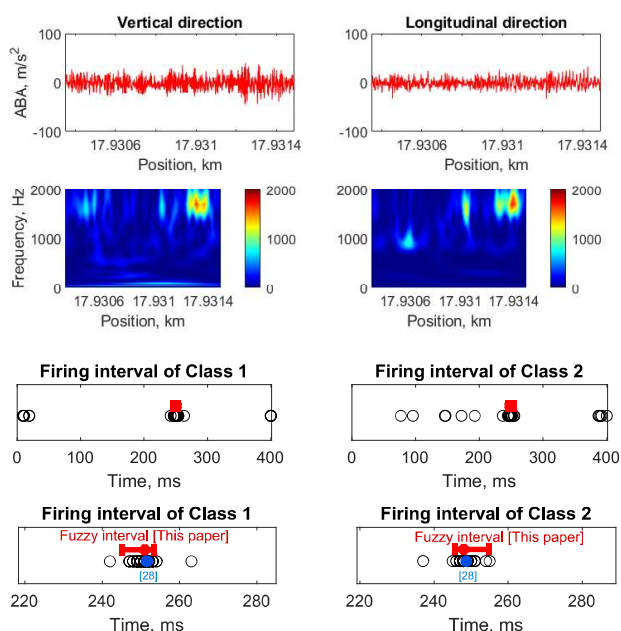


Fig. 8: Predictive result of sample 4th that is correctly predicted as nondefective rail with 16.0% of prediction certainty and do not agree with prediction results from [28].

[9] A. Cicirello and F. Giunta, "Machine learning based optimization for interval uncertainty propagation," *Mechanical Systems and Signal Processing*, vol. 170, p. 108619, 2022.

[10] Z. Deng, Z. Guo, and X. Zhang, "Interval model updating using perturbation method and radial basis function neural networks," *Mechanical Systems and Signal Processing*, vol. 84, pp. 699–716, 2017.

[11] L. Wang, Z. Chen, and G. Yang, "An interval uncertainty analysis method for structural response bounds using feedforward neural network differentiation," *Applied Mathematical Modelling*, vol. 82, pp. 449–468, 2020.

[12] A. Khosravi and S. Nahavandi, "Combined nonparametric prediction intervals for wind power generation," *IEEE Transactions on Sustainable Energy*, vol. 4, pp. 849–856, 2013.

[13] I. Škrjanc, "Confidence interval of fuzzy models: An example using a waste-water treatment plant," *Chemometrics and Intelligent Laboratory Systems*, vol. 96, pp. 182–187, 2009.

[14] —, "Fuzzy confidence interval for ph titration curve," *Applied Mathematical Modelling*, vol. 35, pp. 4083–4090, 2011.

[15] L. Maciel, F. Gomide, and R. Ballini, "Evolving possibilistic fuzzy modeling for financial interval time series forecasting," *2015 Annual Conference of the North American Fuzzy Information Processing Society (NAFIPS) held jointly with 2015 5th World Conference on Soft Computing (WConSC)*, pp. 1–6, 2015.

[16] L. Maciel, R. Ballini, and F. Gomide, "Adaptive fuzzy modeling of interval-valued stream data and application in cryptocurrencies prediction," *Neural Computing and Applications*, 2021.

[17] D. Leite, P. Costa, and F. Gomide, "Evolving granular neural networks from fuzzy data streams," *Neural Networks*, vol. 38, pp. 1–16, 2013.

[18] L. G. Marín, N. Cruz, D. Sáez, M. Sumner, and A. Núñez, "Prediction interval methodology based on fuzzy numbers and its extension to fuzzy systems and neural networks," *Expert Systems with Applications*, vol. 119, pp. 128–141, 2019.

[19] F. Valencia, J. Collado, D. Sáez, and L. G. Marín, "Robust energy management system for a microgrid based on a fuzzy prediction interval model," *IEEE Transactions on Smart Grid*, vol. 7, pp. 1486–1494, 2016.

[20] D. Sáez, F. Ávila, D. Olivares, C. Cañizares, and L. Marín, "Fuzzy prediction interval models for forecasting renewable resources and loads in microgrids," *IEEE Transactions on Smart Grid*, vol. 6, pp. 548–556, 2015.

[21] S. L. Ho, M. Xie, L. C. Tang, K. Xu, and T. N. Goh, "Neural network modeling with confidence bounds: A case study on the solder paste deposition process," *IEEE transactions on electronics packaging manufacturing*, vol. 24, pp. 323–332, 2001.

[22] A. Kavousi-Fard, A. Khosravi, and S. Nahavandi, "Reactive power compensation in electric arc furnaces using prediction intervals," *IEEE transactions on industrial electronics*, vol. 64, pp. 5295–5304, 2017.

[23] J. Pang, D. Liu, Y. Peng, and X. Peng, "Optimize the coverage probability of prediction interval for anomaly detection of sensor-based monitoring series," *Sensors*, vol. 18, pp. 967–991, 2018.

[24] I. Škrjanc, S. Blažič, and O. Agamennoni, "Identification of dynamical systems with a robust interval fuzzy model," *Automatica*, vol. 41, pp. 327–332, 2005.

[25] A. Jamshidi, A. Núñez, R. Dollevoet, and Z. Li, "Robust and predictive fuzzy key performance indicators for condition-based treatment of squats in railway infrastructures," *Infrastructure Systems*, vol. 23, p. 04017006, 2017.

[26] A. Jamshidi, S. Hajizadeh, Z. Su, M. Naeimi, A. Núñez, R. Dollevoet, B. D. Schutter, and Z. Li, "A decision support approach for condition-based maintenance of rails based on big data analysis," *Transportation Research Part C: Emerging Technologies*, vol. 95, pp. 185–206, 2018.

[27] S. M. Bohte, J. N. Kok, and H. L. Poutré, "Error-backpropagation in temporally encoded networks of spiking neurons," *Neurocomputing*, vol. 48, pp. 17–37, 2002.

[28] W. Phusakulkajorn, J. Hendriks, Z. Li, and A. Núñez, "Spiking neural network with time-varying weights for detection of rail squats," *under review*.

[29] A. Núñez, A. Jamshidi, and H. Wang, "Pareto-based maintenance decisions for regional railways with uncertain weld conditions using the hilbert spectrum of axle box acceleration," *IEEE Transactions on Industrial Informatics*, vol. 15, pp. 1496–1507, 2019.

[30] Z. Su, A. Jamshidi, A. Núñez, S. Baldi, and B. D. Schutter, "Multi-level condition-based maintenance planning for railway infrastructures – a scenario-based chance-constrained approach," *Transportation Research Part C: Emerging technologies*, vol. 84, pp. 92–123, 2017.

[31] —, "Integrated condition-based track maintenance planning and crew scheduling of railway networks," *Transportation Research Part C: Emerging technologies*, vol. 105, pp. 359–384, 2019.

[32] W. Maass, "Networks of spiking neurons: The third generation of neural network models," *Neural Networks*, vol. 10, pp. 1659–1671, 1997.

[33] S. Ghosh-Dastidar and H. Adeli, "A new supervised learning algorithm for multiple spiking neural networks with application in epilepsy and seizure detection," *Neural Networks*, vol. 22, pp. 1419–1431, 2009.

[34] O. Booi and H. T. Nguyen, "A gradient descent rule for multiple spiking neurons emitting multiple spikes," *Information Processing Letters*, vol. 95, pp. 552–558, 2005.

[35] J. J. Wade, L. J. McDaid, J. A. Santos, and H. M. Sayers, "SWAT: A spiking neural network training algorithm for classification problems," *IEEE Transactions on neural networks*, vol. 21, pp. 1817–1830, 2010.

[36] H. Shao, H. Jiang, H. Zhang, W. Duan, T. Liang, and S. Wu, "Rolling bearing fault feature learning using improved convolutional deep belief network with compressed sensing," *Mechanical Systems and Signal Processing*, vol. 100, pp. 743–765, 2018.

[37] C. Tan, M. Šarlija, and N. Kasabov, "NeuroSense: Short-term emotion recognition and understanding based on spiking neural network modelling of spatio-temporal EEG patterns," *Neurocomputing*, vol. 434, pp. 137–148, 2021.

[38] Z. Yan, J. Zhou, and W. F. Wong, "Energy efficient ECG classification with spiking neural network," *Biomedical Signal Processing and Control*, vol. 63, p. 102170, 2021.

[39] R. E. Turkson, H. Qu, C. B. Mawuli, and M. J. Eghan, "Classification of Alzheimer's disease using deep convolutional spiking neural network," *Neural Processing Letters*, vol. 53, pp. 2649–2663, 2021.

[40] A. Jeyasothy, S. Sundaram, and N. Sundararajan, "SEFRON: A new spiking neuron model with time-varying synaptic efficacy function for pattern classification," *IEEE Transactions on Neural Networks and Learning Systems*, vol. 30, pp. 1231–1240, 2019.

[41] M. Molodova, Z. Li, A. Núñez, and R. Dollevoet, "Parametric study of the axle box acceleration at squats," *Proceedings of the Institution of Mechanical Engineers Part F: Journal of Rail and Rapid Transit*, vol. 229, pp. 841–851, 2015.

[42] Z. Wei, A. Núñez, Z. Li, and R. Dollevoet, "Evaluating degradation at railway crossings using axle box acceleration measurements," *Sensors*, vol. 17, p. 2236, 2017.